Green Chemistry

Accepted Manuscript

This article can be cited before page numbers have been issued, to do this please use: G. Pomalaza, G. Vofo, M. Capron and F. Y. Dumeignil, *Green Chem.*, 2018, DOI: 10.1039/C8GC01211C.

ROYAL SOCIETY OF CHEMISTRY

rsc.li/green-chem

View Article Online
DOI: 10.1039/C8GC01211C

Green Chemistry

COMMUNICATION

ZnTa-TUD-1 as easily prepared, highly efficient catalyst for the selective conversion of ethanol to *1,3*-butadiene

G. Pomalaza,[a] G. Vofo,[a] M. Capron[a] and F. Dumeignil[a,*]

Received 00th January 20xx,
Accepted 00th January 20xx

DOI: 10.1039/x0xx00000x

www.rsc.org/

High performances in the conversion of ethanol to *1,3*-butadiene were achieved with a Zn(II) and Ta(V) catalyst supported on TUD-1, a mesoporous silica. Selectivity reached 73% after 3 h at 94% conversion. At increased ethanol flow, initial productivity rose to 2.45 $g_{1,3\text{-BD}}.g_{cat}^{-1}.h^{-1}$, which remained stable during 60 h on stream, making it the most productive catalyst according to the literature. Preliminary characterization suggests morphological and acid properties contribute to these exceptional performances.

Introduction

1,3-butadiene (herein referred to as *1,3*-BD) is considered the most economically important unsaturated C_4 compound; it is indeed crucial to the manufacturing of several polymers, such as synthetic rubber.[1,2] *1,3*-BD is predominantly extracted from the C_4 fraction following ethylene manufacturing *via* the steam cracking of naphtha.[1,2] Because of scarcity issues and environmental concerns, sustainable on-purpose production methods for *1,3*-BD are of topical interest. Bioethanol can be obtained from renewable sources.[3] For this reason, the catalytic conversion of ethanol (EtOH) to *1,3*-BD is attracting much attention, despite being an old technology.[4] Recent research has focused on increasing *1,3*-BD yield and productivity through catalyst design, with the aim of turning the ethanol-to-butadiene (ETB) reaction into an economically viable process.[5]

Owing to its complex mechanism (Figure 1), the ETB reaction requires multifunctional catalysts; most illustrated steps occur on different catalytic sites, generally provided by combining metals and/or metal oxides possessing the appropriate chemical properties. For instance, acid sites are suitable for the aldol coupling and dehydration reactions (steps B, C and E in Figure 1).[6,7] Ethanol dehydrogenation and aldol coupling, also

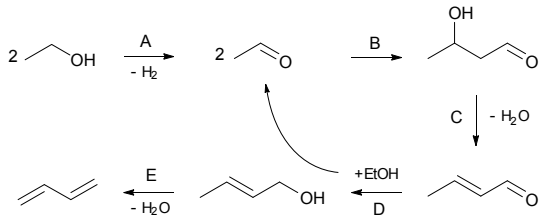

Figure 1 Main reaction pathway leading to *1,3*-butadiene. Reaction steps are: (A) ethanol dehydrogenation; (B) aldol condensation; (C) dehydration; (D) Meerwein–Ponndorf–Verley-Oppenaur (MPVO) reaction; (E) dehydration.[6]

known as aldolization (steps A and B in Figure 1) can occur on basic sites.[8,9] Metal nanoparticles are also suitable for step A.[10] Furthermore, maximizing *1,3*-BD formation necessitates a catalyst with an adequate balance of such properties.[11] Otherwise, alternative reaction pathways may be favoured, leading to the formation of undesired by-products, such as ethylene or butanol.[12]

Recent improvements in the design of catalysts for the ETB reaction have yielded high-performing materials.[4] The combination of supported Lewis-acidic metal oxides [Zr(IV), Hf(IV), Ta(V) or Nb(V)] with dehydrogenation promoters (Ag, Cu) has afforded highly active catalysts.[13–15] The use of mesoporous catalyst carriers was also demonstrably increased catalytic stability and *1,3*-BD selectivity.[14,16,17] Recently, Lee *et al*. designed a highly selective and stable zirconia catalyst supported on mesocellular siliceous foam.[14] They attributed the performances of their catalyst to two factors: *(i)* uniform tridimensional mesoporous supports, enabling efficient mass transfer and excellent resistance to coke, and *(ii)* highly dispersed active metal oxides. The benefits of mesoporous morphology to the catalytic performances were also observed by others.[16–18] Yet, this strategy is underutilized, with many recent works preferring tried-and-tested microporous zeolite supports, such as dealuminated zeolite beta.[13,19] Perhaps the time-consuming synthesis of mesoporous materials, such as mesocellular siliceous foam and SBA-15, including the post-

[a] Univ. Lille, CNRS, Centrale Lille, ENSCL, Univ. Artois, UMR 8181 - UCCS - Unité de Catalyse et Chimie du Solide, F-59000 Lille, France.
* Corresponding author: franck.dumeignil@univ-lille.fr
† Footnotes relating to the title and/or authors should appear here.
Electronic Supplementary Information (ESI) available: [details of any

View Article Online
DOI: 10.1039/C8GC01211C

synthesis modifications needed to introduce an active phase, hinders their use and study.

In this work, we report the facile preparation and study of a Zn(II) and Ta(V) catalyst supported on mesoporous TUD-1, achieving the aforementioned high performance-driving factors highlighted by Lee *et al.*[14] TUD-1 is a sponge-like mesoporous silica with an irregular three-dimensional pore system.[20] This material has found many applications as a support for heterogeneous catalysts due to its numerous practical advantages. Its structural properties are easily tuned following the preparation of a precursor gel by adjusting the duration of its hydrothermal treatment. This way, siliceous foam with mesopores ranging from 2 to 20 nm and with specific surface areas between 300 and 900 m^2/g can be obtained. Furthermore, metals or metal oxides are easily dispersed within the silica framework through a simple modification of the one-pot synthesis. This way, bimetallic or bi-metal oxide systems are effortlessly synthesized to take advantage of synergetic effects between two different active phases.[20] In addition, TUD-1 catalysts are usually highly active while showing a remarkable hydrothermal stability.[20–25] The key to TUD-1's versatility and straightforward preparation is the use of a chelating agent during the gelification process, which doubles as a structure directing agent. By chelating precursor ions prior to gelification, it also ensures an excellent degree of dispersion during the oxidizing calcination, which frees the agent and condenses the silica, simultaneously generating mesopores *via* steric hindrance.

Although both Zn(II) and Ta(V) have been used separately in other ETB catalysts, they are seldom reported together. Zinc oxide is cited as a promoter of ethanol dehydrogenation.[26,27] Tantalum oxide was shown to reach remarkable selectivity when converting mixtures of ethanol with acetaldehyde.[16,28,29] In the present work, when supported on TUD-1, stable *1,3*-BD selectivity peaking at 73 % for an EtOH conversion of 96% was achieved (T: 400 °C, $WHSV_{EtOH}$: 5.3 h^{-1}, TOS: 3 h). Productivity is also exceptionally high and stable, despite the high ethanol flow employed, outperforming any other formulation disclosed so far in the direct conversion to *1,3*-BD under comparable conditions.

Experimental

Catalysts preparation

A catalyst consisting of Zn(II) and Ta(V) supported on TUD-1 (labelled ZnTa-TUD-1) was synthesized with tetraethylene glycol as a chelating agent in a one-pot procedure based on a sol-gel methodology as found in the literature.[24] The appropriate amounts of Zn and Ta salts (zinc acetate dehydrate and tantalum ethoxide) were first dissolved in absolute ethanol with a Zn:Ta molar ratio of 1.5. Tetraethyl orthosilicate (TEOS) was added drop-wise to the ethanol solution while stirring. The chelating agent was subsequently added in a similar fashion. After 1 h of stirring, an aqueous solution of tetraethyl ammonium hydroxide (35 wt.%) was added dropwise to the mixture under vigorous stirring, which was maintained for 2 h. A clear gel was obtained and left to age at room temperature for 24 h. The aged gel was dried at 100 °C for 24 h before being gently ground to a white powder and subjected to a hydrothermal treatment in a Teflon-lined stainless-steel autoclave for 24 h at 180 °C. The resulting brown powder was calcined at 600 °C in a tubular quartz reactor for 10 h with a temperature ramp of 1 °C.min^{-1} and an air flow of 0.3 L.min^{-1}. A fine white powder was ultimately recovered.

For comparison, additional catalysts with the same amounts of Zn and Ta were prepared. In one case, zeolite BEA from Zeolyst international (CP814C) was dealuminated following a procedure detailed in the literature.[30] In another, fumed silica (Alfa Aeser) was used. In both cases, the appropriate amounts of Zn and Ta were introduced *via* incipient wetness impregnation (IWI) using the same precursor salts as those used in the preparation of the TUD-1-based catalyst. Drying and calcination according to the procedure described above followed, resulting in white powders in both cases. The as-obtained benchmark catalysts were labelled ZnTa/deBEA and ZnTa/SiO_2, respectively.

Catalyst testing

Catalytic activity tests were carried out with a Multi-R® apparatus from Teamcat Solutions SAS.[31] Multi-R® is a high-throughput equipment for heterogeneous catalysts screening. This device consists of 3 main components: the feed, the reaction section and the analytical system. The gaseous feed is split and fed into 4 reactors using a splitter provided by the manufacturer. The machine is adjusted so that every reactor receives an equal inlet flow in terms of gas composition and flowrate. Catalysts are loaded in specific liners with sintered glass filters and inserted in the device, acting as fixed-bed reactors. The temperature of each reactor is controlled independently. Their output is analysed with an online GC (Agilent 7890 A) equipped with a FID detector calibrated to detect and quantify the major products of the reaction, *i.e. 1,3*-BD, acetaldehyde (AcH), ethylene ($C_{2=}$), propylene, etc.). Choosing from the output of one reactor to another is done by an independently controlled valve.

Reaction temperature was set at 400 °C with a pressure of 1 atm. Catalysts were ground and sieved to 120 mesh-sized granules; 30 mg of catalyst were loaded in the glass reactors and held in place using SiC. Ethanol was introduced into the splitter and then each reactor by passing helium through a bubbler containing ≥ 99.8 % ethanol maintained at 25 °C. EtOH vapour concentration was set at 4.5 vol.%. Helium flow and catalyst mass were adjusted to provide a weighted hourly space velocity ($WHSV_{EtOH}$) of 2, 5.3 and 8 h^{-1}.

Catalyst regeneration was carried out in the same reactor, under synthetic air with a flow of 10 mL.min^{-1} for a period of 6 hours at 400 °C.

Catalytic activity was characterized by the conversion of ethanol (X, %), the selectivity towards each product (S_i, %), the molar yield of each product (Y_i, %) and the productivity in *1,3*-BD ($P_{1,3\text{-BD}}$, $g_{1,3\text{-BD}}.g_{cat}^{-1}.h^{-1}$). Each value was calculated according to the following formulas:

View Article Online
DOI: 10.1039/C8GC01211C

$$X=\frac{c^0_{EtOH}-c_{EtOH}}{c^0_{EtOH}}\cdot 100$$

$$S_i=\frac{c_i}{c^0_{EtOH}-c_{EtOH}}\cdot 100$$

$$Y_i=X\cdot S_i$$

$$P_{1,3\text{-BD}}=X\cdot S_{1,3\text{-BD}}\cdot WHSV_{EtOH}\cdot 0.587/100$$

Where c_{EtOH} is the amount of carbon moles from EtOH entering the reactor, c_i is the amount of carbon moles detected for a given product *i*, the 0.587 coefficient represents the 100 % mass yield of butadiene and $WHSV_{EtOH}$ represents the mass flow of ethanol per mass of catalysts (expressed as $g_{EtOH}.g_{cat}^{-1}.h^{-1}$). The carbon balance (*CB*) for each test was calculated by dividing the sum of carbon moles detected with the molar amount of carbon introduced as EtOH in percentage.

Characterization

Physisorption experiments were performed at −196 °C on a Micromeritics Tristar II instrument. Before analysis, a known mass of solid (~ 50–200 mg) was outgassed under vacuum at 150 °C for 6 h. Specific surface area (S_{BET}) could then be calculated using the B.E.T. equation on the linear part of the B.E.T. plot (P/P_0=0.1–0.25). Average pore volume (V_p) was measured from the adsorption branch of the isotherm, at a P/P_0 value of 0.98. The mean pore diameter (D_p) was calculated by applying the Barrett-Joyner-Halenda model on the desorption branch of the isotherm.

Powder X-ray diffraction (XRD) high angles patterns were recorded on a Bruker AXS D5005 diffractometer using a CuK_α radiation (λ = 1.54184 Å) as an X-ray source in the 2ϑ range from 10 to 50° with a step of 0.05° (integration time of 8 s).

Elemental analysis was performed with the catalysts using inductively coupled plasma-optic emission spectroscopy 720-ES ICP-OES (Agilent) with axial viewing and simultaneous CCD detection. The quantitative determination of metal content in the catalysts was made based on the analysis of certificated standard solution. The analytes were prepared by dissolving 10 mg of dried and ground catalyst samples in concentrated acid (HF:HNO_3=1:3, v:v). Each sample solution was stirred overnight in an ultrasonic cleaner heated to 50 °C before dilution in 20 mL of ultrapure water and analysis.

Acid sites were quantified using NH_3-temperature programmed desorption (NH_3-TPD). The measurements were performed on calcined samples of known masses with a Micrometrics Autochem 2920 apparatus coupled with a Pfeiffer mass spectrometer (MS). NH_3 adsorption was performed at room temperature during 30 min using a NH_3 flow consisting of 5 % NH_3 in 95 % He). Desorption was performed until 900 °C (ramp of 10 °C.min^{-1}) and held for 30 min in He (30 mL.min^{-1}).

Results & Discussion

Table 1 Catalytic performances of Zn(II) and Ta(V) on TUD-1, dealuminated BEA and SiO_2 in *1,3*-BD production at 400 °C, $WHSV_{EtOH}$ of 5.3 h^{-1} after 3 h.

Sample	*X*, %	$S_{1,3\text{-BD}}$, %	S_{AcH}, %	$S_{C2=}$, %	$Y_{1,3\text{-BD}}$, %	$P_{1,3\text{-BD}}$, [a]	*CB*, %
ZnTa-TUD-1	94	73	18	10	69	2.13	102
ZnTa/deBEA	95	59	25	8	56	1.74	95
ZnTa/SiO_2	94	48	34	4	45	1.40	95

[a] *1,3*-Butadiene productivity in $g_{1,3\text{-BD}}.g_{cat}^{-1}h^{-1}$.

Table 2 Metal loading and molar ratio in the studied samples.

Sample	Si/Zn	Si/Ta	Zn/Ta	Formula
ZnTa-TUD-1	16.5	29.6	1.79	$Zn_{6.1}Ta_{3.4}$-TUD-1
ZnTa/deBEA	18	30.3	1.67	$ZnT_{5.6}Ta_{3.3}$/deBEA
ZnTa/SiO_2	19.2	31	1.61	$Zn_{5.2}Ta_{3.2}$/SiO_2

We benchmarked the performances of ZnTa-TUD-1 in terms of *1,3*-BD selectivity and *1,3*-BD productivity against those of common materials: abundant publications on the Lebedev process employ dealuminated zeolite and silica-supported catalysts prepared through impregnation. *1,3*-BD selectivity demonstrably reflected the suppression of undesired byproducts, the presence of which being detrimental to the viability of bio-based processes.[32] Productivity is also hailed as an important indicator of industrial relevancy, unproductive catalysts obviously preventing a robust economic viability.[33] Carbon balance was within 95 and 105% over the course of the experiments and considered as satisfactory. The results are reported in Table 1.

EtOH conversion was equally high on all the catalysts, reaching 94-95%. *1,3*-BD selectivity depended on the catalyst, peaking at 73 % over ZnTa-TUD-1. This value is relatively high considering the elevated ethanol flow ($WHSV_{EtOH}$: 5.3), most articles reporting experimental conditions below 2 h^{-1}.[4] Conversely, selectivity over ZnTa/deBEA and ZnTa/SiO_2 was respectively 10 and 20 percentage points smaller. This disparity was mirrored in the higher selectivity towards AcH observed with both. These remarkable results are ostensibly attributed to the choice of catalyst carrier, possibly to its intrinsic properties or its synthesis procedure. To adequately investigate this assumption, the three samples were prepared with equal amounts of Zn(II) and Ta(V). Elemental analysis of Si, Ta and Zn in the prepared catalysts was conducted using ICP-OES, indicating that all the three catalysts containing similar amounts of oxide phase and Zn/Ta ratio (Table 2). This excludes the possibility that the performance difference observed stemmed from uneven amounts of active phases.

Carrier morphology has been shown to influence catalytic activity in the ETB reaction. Jones *et al*. observed an increase in *1,3*-BD selectivity by up to 17 percentage points when the pore size diameter of a silica support was increased from 6 nm to

View Article Online
DOI: 10.1039/C8GC01211C

15 nm.[17] Likewise, Chae *et al.* also noted an initial benefit to increasing pore size diameter from 2.5 nm to 10.9 nm when using SBA-15 as a catalyst carrier. However, these became modest after 10 h on stream due to deactivation.[16] As stipulated by Lee *et al*., large and uniform pore sizes contribute to a stable catalytic activity.[14] Furthermore, Jones *et al*. also have drawn a direct correlation between specific surface area and *1,3*-BD yield.[34,35] These observations highlight the importance physical properties have in the ETB reaction, which were promptly investigated. Table 3 summarizes the results obtained by N_2 physisorption regarding the morphology of the catalysts prepared. ZnTa-TUD-1 possessed the expected morphological features: a large specific surface area (300-900 $m^2.g^{-1}$), a large porous volume and mesopores (2-20 nm).[20] Figure S1 indicates that the pore size distribution is uniform, peaking at around 18 nm, with a full width at half maximum of 6.2 nm. Conversely, ZnTa/deBEA had a large specific surface, but smaller pore volume and diameter, the distribution of which was uneven. Figure S1 illustrates how it ranges from nanopores inherent to zeolitic materials to mesopores formed during the dealumination process. ZnTa/SiO_2 had larger average pore diameter compared to the TUD-1 sample, but much smaller specific surface area and pore volume. Part of the inferior performances can be attributed in part to a lack of uniform mesopores in the case of zeolite-supported catalyst and the smaller specific surface area of the silica-supported catalyst. However, other factors should also be taken in consideration.

Sushkevich and Ivanova have identified a direct correlation between the amount of Zr(IV) Lewis acid sites and the *1,3*-BD rate of formation.[13] In their study of the reaction mechanism, they propose that Lewis acid sites such as those brought by Ta(IV) catalyze every reaction step subsequent to the initial ethanol dehydrogenation step (aldol condensation, MPVO reaction and alcohol dehydration).[6] Since aldol condensation has been identified as the rate-limiting step, the observed accumulation of AcH suggests that the disparity in selectivity is related to the acidic Ta(V) phase. The amount and strength of acidic sites on the three catalysts were characterized by NH_3-TPD. Desorption profiles are illustrated in Figure S2 and the results are summarized in Table 4. Figure S2 suggests the existence of a single type of acid sites covering a broad range of strengths in each catalyst, as evidenced by the single broad peaks at 260 °C. The combination of Zn(II) with Ta(V) may explain the absence of acid sites desorbing at higher temperatures, *i.e.*, of stronger acid sites; some authors have reported a passivation of strong acidity upon the introduction of zinc oxide.[15,36] Despite containing equal amounts of Ta and Zn, the total amount of acid sites per gram differed according to the catalyst carrier used. ZnTa-TUD-1 possessed the double of acid sites than ZnTa/deBEA and five times more than ZnTa/SiO_2.

A correlation between the amount of acid sites and selectivity towards *1,3*-BD after 3 h on stream was observed (Figure 2). Considering that silicate-supported Ta(IV) is predominantly Lewis acidic when reacting with alcohols, these results are in line with the current theory regarding the ETB mechanism.[29] The amount of Ta being identical on each

Table 3 Morphological properties obtained by N_2 physisorption.

Sample	S_{BET}[a], $m^2.g^{-1}$	Pore vol.[a], $cm^3.g^{-1}$	Average pore diameter, nm
ZnTa-TUD-1	640	2.20	13.6
ZnTa/deBEA	501	0.60	6.0
ZnTa/SiO_2	185	0.82	16.05

[a] Specific surface area [b] Pore volume, measured at P/P_0 = 0.98.

Table 4 Amount of acid sites measured by NH_3-TPD expressed by weight and surface units

Sample	Nb of acid sites per weight ($mmol.g^{-1}$)	N° of acid sites per surface ($mmol.m^{-2}$)
ZnTa-TUD-1	0.88	563
ZnTa/deBEA	0.43	213
ZnTa/SiO_2	0.17	30

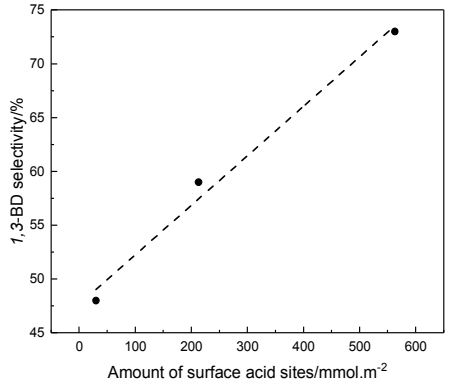

Figure 2 Correlation curve between 1,3-BD selectivity (T: 400 °C, $WHSV_{EtOH}$: 5.3 h^{-1}, P: 1 atm, TOS: 3 h) and total surface acidity.

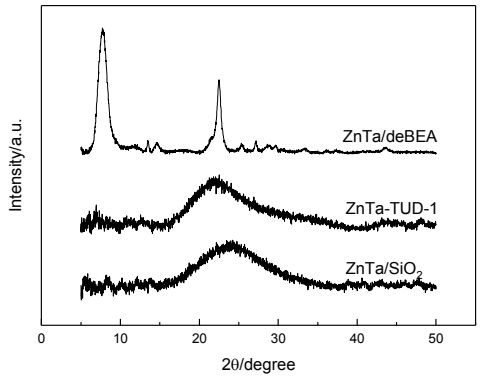

Figure 3 XRD patterns of synthesized Zn(II) & Ta(V) catalysts

View Article Online
DOI: 10.1039/C8GC01211C

catalyst, this suggests that the dispersion was more successful using the TUD-1 methodology—thereby creating more isolated acid sites. ZnTa/deBEA was prepared using a method that generates isolated Ta(V) sites. However, it was successfully reported for Ta wt.% of 1, 2 and 3.[29,37] In this work, the Ta loading reaches 10 wt.%, which may have proved too much for proper dispersion using IWI. TUD-1 synthesis appears to be better suited for dispersing high active phase loadings.

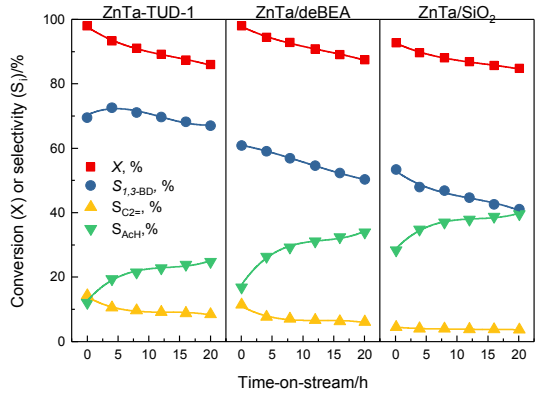

Figure 4 Performances of ZnTa-TUD-1 , ZnTa/deBEA and ZnTa/SiO_2 over a 20 h period (T: 400 °C, $WHSV_{EtOH}$: 5.3 h^{-1}, P: 1 atm).

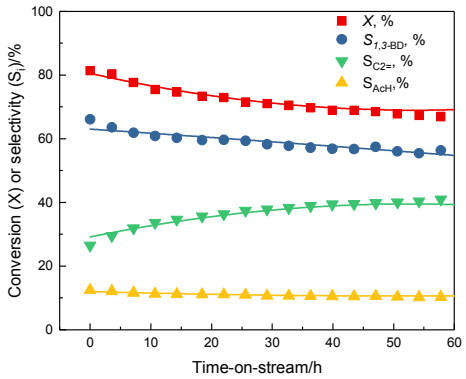

Figure 5 Stability of ZnTa-TUD-1 at $WHSV_{EtOH}$ 8 h^{-1} (T: 400 °C, $WHSV_{EtOH}$: 8 h^{-1}, P: 1 atm).

Powder XRD diffractograms of the synthesized samples (Figure 3) did not show the presence of bulk crystalline ZnO or Ta_2O_5, suggesting only an absence of large extra framework metal oxides particles. In addition, the diffractograms of ZnTa-TUD-1 and ZnTa/SiO_2 both possessed the broad bands around 15-30°, common on amorphous siliceous materials. Bands typical of the BEA structure on the diffractogram of ZnTa/deBEA—similar to those observed with other Ta-containing dealuminated BEA—confirms that the carrier retained its zeolite framework throughout the dealumination and impregnation processes.[37]

Additional tests with the three synthesized materials were conducted to measure their stability, as deactivation commonly plagues the performances of ETB catalysts. Figure 4 compares the conversion and selectivity to the three major products over ZnTa-TUD-1, ZnTa/deBEA and ZnTa/SiO_2 over 20 h of reaction. Each catalyst suffered from a similar loss of activity in converting EtOH (about 10 percentage points in 20 h). The *1,3*-BD selectivity also dropped over time, with AcH selectivity increasing as a result, suggesting that coke deposits gradually poison the active acid sites. The rate of deactivation in terms of *1,3*-BD selectivity depended on the material. ZnTa-TUD-1 fell 7 percentage points over 20 h, whereas ZnTa/deBEA and ZnTa/SiO_2 decreased by 13 and 12 percentage points, respectively. Ostensibly, the stability of the TUD-1 catalyst is attributable to its uniform, three-dimensional mesopores.[14]

Having demonstrated both superior activity and stability, ZnTa-TUD-1 was further tested to evaluate its performances under different conditions. First, the effect of $WHSV_{EtOH}$ was evaluated. As illustrated by Figure S3, ethanol conversion, as well as *1,3*-BD and ethylene selectivity decrease as function of $WHSV_{EtOH}$, while AcH selectivity increases. These results are consistent with the model developed by Jones, Pinto *et al*. regarding the effect of reaction conditions on catalytic activity.[38] The accumulation of AcH with increased $WHSV_{EtOH}$ is also consistent with the conclusions that aldol condensation is the rate-limiting step on solid acids.[6]

Deactivation of ZnTa-TUD-1 was again tested. At $WHSV_{EtOH}$ of 8 h^{-1}, *1,3*-BD selectivity was initially 66%, losing 13 percentage points over the course of 60 hours (Figure 5). Ethanol conversion also decreased by 15 percentage points, whereas AcH selectivity grew steadily to around 35% before stabilizing at around TOS of 40 h. At TOS of 3 h, *1,3*-BD productivity is 2.45 $g_{1,3\text{-BD}}.g_{cat}^{-1}.h^{-1}$. A preliminary regeneration attempt was conducted at 400 °C under air in an attempt to remove coke deposits responsible for deactivation. Figure S4 illustrates how ethanol conversion, acetaldehyde selectivity and ethylene selectivity were returned to their initial values. However, *1,3*-BD selectivity was only partially recovered and continued the trend of deactivation following 15 hours of reaction under the same conditions. These results suggest that carbonaceous species are partly responsible for the loss of catalytic activity. With regards to *1,3*-BD selectivity, deactivation may either be caused by species requiring different, possibly harsher calcination conditions or that the nature of the active site is compromised during the reaction/regeneration procedure. Work is ongoing to understand this phenomenon and to design an optimized regeneration step.

Compared to the performances reported in the literature, ZnTa-TUD-1 fared well: the other two most productive ETB catalysts (hierarchical MgO-SiO_2 from Men *et al*. and ZnY/deBEA from Li *et al*.) lost their selectivity toward *1,3*-BD faster than ZnTa-TUD-1.[19,39] Starting with a *1,3*-BD selectivity of 77%, MgO-SiO_2 (T: 450 °C, $WHSV_{EtOH}$: 4.1 h^{-1}) lost 13 percentage points in 20 h.[39] ZnY/deBEA (T: 400 °C, $WHSV_{EtOH}$: 7.9 h^{-1}) decreased by 20 percentage points in 10 h from an initial selectivity of 63%.[19] Figure S5 illustrates the productivity of the three catalysts as the reaction progresses. Figure S6 compares *1,3*-BD productivity observed on ZnTa-TUD-1 with

View Article Online
DOI: 10.1039/C8GC01211C

the other top 10 most productive catalysts found in the literature at the different $WHSV_{EtOH}$ each were tested. Admittedly, the difference in reaction conditions makes a direct comparison partiality inaccurate, as we have demonstrated that $WHSV_{EtOH}$ affects catalytic performances. Nevertheless, these figures indicate that ZnTa-TUD-1 is the most selective and stable catalyst at high ethanol flow, boasting a *1,3*-BD productivity of 2.45 $g_{1,3\text{-BD}}.g_{cat}.h^{-1}$ after 3 hours. To the best of our knowledge, this makes it the most productive catalyst recorded so far.

Conclusions

ZnTa-TUD-1 was revealed as a highly selective catalyst for the conversion of ethanol to *1,3*-butadiene. Its simple preparation method allows us, in a one-pot operation, both to disperse the active phase within the support and to generate a mesoporous morphology beneficial to its catalytic activity. This does away with pre and post-synthesis procedures commonly used for introducing metal oxides such as ion-exchange, mechanical mixing, urea hydrolysis or impregnation[13,14,19], but also for generating mesopores, such as zeolites dealumination. In addition, the mesopores are formed using environmentally friendly chelating agents that double as structure-directing agents.

A remarkable selectivity towards BD of 73% was observed with ZnTa-TUD-1 after 3 h on stream at 400 °C, which was tied with the total amount of surface acid sites. Using a $WHSV_{EtOH}$ of 5.3 h^{-1} combined with the aforementioned selectivity, a *1,3*-BD productivity reaching 2.13 $g_{1,3\text{-BD}}.g_{cat}.h^{-1}$ was attained. Raising the $WHSV_{EtOH}$ to 8 h^{-1} decreased *1,3*-BD yield, but increased overall *1,3*-BD productivity to 2.45 $g_{1,3\text{-BD}}.g_{cat}.h^{-1}$, an unprecedented value according to the literature. Because productivity is considered a key factor in making the ETB process compete with petroleum-derived *1,3*-butadiene, these performances are very promising and important. Additionally, the catalyst proved to be remarkably stable for a period of 60 hours—a phenomenon ostensibly attributed to its morphology.[14] Regeneration under air to remove deposed carbonaceous species was only partially successful, but is undergoing improvements.

Further synthesis is ongoing to optimize the highly tuneable TUD-1 catalyst. Additionally, a complete characterization of the catalytic system is in progress to fully grasp how its physicochemical properties are tied to the performances observed.

Acknowledgments

Authors acknowledge the support from the French National Research Agency (ANR-15-CE07-0018-01). Chevreul Institute (FR 2638), Ministère de l'Enseignement Supérieur, de la Recherche et de l'Innovation, Région Hauts-de-France and FEDER are acknowledged for supporting and funding partially this work.

Conflicts of interest

There are no conflicts to declare.

Notes and references

1 M. Dahlmann, J. Grub and E. Löser, in *Ullmann's Encyclopedia of Industrial Chemistry*, Wiley-VCH Verlag GmbH & Co. KGaA, Weinheim, Germany, 2011, vol. 100 C, pp. 1–24.
2 H. N. Sun and J. P. Wristers, in *Kirk-Othmer Encyclopedia of Chemical Technology*, John Wiley & Sons, Inc., Hoboken, NJ, USA, 2002, vol. 4.
3 N. Kosaric, Z. Duvnjak, A. Farkas, H. Sahm, S. Bringer-Meyer, O. Goebel and D. Mayer, in *Ullmann's Encyclopedia of Industrial Chemistry*, Wiley-VCH Verlag GmbH & Co. KGaA, Weinheim, Germany, 2011, pp. 1–72.
4 G. Pomalaza, M. Capron, V. Ordomsky and F. Dumeignil, *Catalysts*, 2016, **6**, 203.
5 M. Jones, *Chem. Cent. J.*, 2014, **8**, 53.
6 V. L. Sushkevich and I. I. Ivanova, *Appl. Catal. B Environ.*, 2017, **215**, 36–49.
7 E. V Makshina, M. Dusselier, W. Janssens, J. Degrève, P. A. Jacobs and B. F. Sels, *Chem. Soc. Rev.*, 2014, **43**, 7917–7953.
8 V. V. Ordomsky, V. L. Sushkevich and I. I. Ivanova, *J. Mol. Catal. A Chem.*, 2010, **333**, 85–93.
9 A. Chieregato, J. Velasquez Ochoa, C. Bandinelli, G. Fornasari, F. Cavani and M. Mella, *ChemSusChem*, 2015, **8**, 377–388.
10 K. I. Shimizu, K. Sugino, K. Sawabe and A. Satsuma, *Chem. - A Eur. J.*, 2009, **15**, 2341–2351.
11 C. Angelici, M. E. Z. Velthoen, B. M. Weckhuysen and P. C. A. Bruijnincx, *Catal. Sci. Technol.*, 2015, **5**, 2869–2879.
12 C. Angelici, M. E. Z. Velthoen, B. M. Weckhuysen and P. C. A. Bruijnincx, *ChemSusChem*, 2014, **7**, 2505–2515.
13 V. L. Sushkevich and I. I. Ivanova, *ChemSusChem*, 2016, **9**, 2216–2225.
14 J. L. Cheong, Y. Shao, S. J. R. Tan, X. Li, Y. Zhang and S. S. Lee, *ACS Sustain. Chem. Eng.*, 2016, **4**, 4887–4894.
15 T. De Baerdemaeker, M. Feyen, U. Müller, B. Yilmaz, F. S. Xiao, W. Zhang, T. Yokoi, X. Bao, H. Gies and D. E. De Vos, *ACS Catal.*, 2015, **5**, 3393–3397.
16 T. W. Kim, J. W. Kim, S. Y. Kim, H. J. Chae, J. R. Kim, S. Y. Jeong and C. U. Kim, *Chem. Eng. J.*, 2014, **278**, 217–223.
17 M. Jones, C. Keir, C. Iulio, R. Robertson, C. Williams and D. Apperley, *Catal. Sci. Technol.*, 2011, **1**, 267.
18 A. Klein and R. Palkovits, *Catal. Commun.*, 2016, **91**, 72–75.
19 W. Dai, S. Zhang, Z. Yu, T. Yan, G. Wu, N. Guan and L. Li, *ACS Catal.*, 2017, **7**, 3703–3706.
20 S. Telalović, A. Ramanathan, G. Mul and U. Hanefeld, *J. Mater. Chem.*, 2010, **20**, 642.
21 L. Li, D. Cani and P. P. Pescarmona, *Inorganica Chim. Acta*, 2015, **431**, 289–296.
22 S. Lima, M. M. Antunes, A. Fernandes, M. Pillinger, M. F. Ribeiro and A. A. Valente, *Molecules*, 2010, **15**, 3863–3877.
23 R. Maheswari, M. P. Pachamuthu and R. Anand, *J. Porous*

View Article Online
DOI: 10.1039/C8GC01211C

Mater., 2012, **19**, 103–110.
24 A. Ramanathan, M. Carmen Castro Villalobos, C. Kwakernaak, S. Telalovic and U. Hanefeld, *Chem. - A Eur. J.*, 2008, **14**, 961–972.
25 W. Yan, A. Ramanathan, P. D. Patel, S. K. Maiti, B. B. Laird, W. H. Thompson and B. Subramaniam, *J. Catal.*, 2016, **336**, 75–84.
26 O. V. Larina, P. I. Kyriienko and S. O. Soloviev, *Catal. Letters*, 2015, **145**, 1162–1168.
27 Y. Hayashi, S. Akiyama, A. Miyaji, Y. Sekiguchi, Y. Sakamoto, A. Shiga, T. Koyama, K. Motokura and T. Baba, *Phys. Chem. Chem. Phys.*, , DOI:10.1039/C6CP04171J.
28 W. J. Toussaint, J. T. Dunn and D. R. Jackson, *Ind. Eng. Chem.*, 1947, **39**, 120–125.
29 P. I. Kyriienko, O. V. Larina, S. O. Soloviev, S. M. Orlyk and S. Dzwigaj, *CATCOM*, 2016, **77**, 123–126.
30 E. Bourgeat-Lami, F. Fajula, D. Anglerot and T. Couriers, *Microporus Mater.*, 1993, **1**, 237–245.
31 WO2015118263 A1, 2015.
32 A. D. Patel, K. Meesters, H. den Uil, E. de Jong, K. Blok and M. K. Patel, *Energy Environ. Sci.*, 2012, **5**, 8430.
33 M. Lewandowski, G. S. Babu, M. Vezzoli, M. D. Jones, R. E. Owen, D. Mattia, P. Plucinski, E. Mikolajska, A. Ochenduszko and D. C. Apperley, *Catal. Commun.*, 2014, **49**, 25–28.
34 S. Da Ros, M. D. Jones, D. Mattia, J. C. Pinto, M. Schwaab, F. B. Noronha, S. A. Kondrat, T. C. Clarke and S. H. Taylor, *ChemCatChem*, 2016, **8**, 2376–2386.
35 J. W. Geus and A. J. Van Dillen, *Prep. Solid Catal.*, 2008, 460–487.
36 R. A. L. Baylon, J. Sun and Y. Wang, *Catal. Today*, 2014, **259**, 446–452.
37 S. Dzwigaj, Y. Millot and M. Che, *Catal. Letters*, 2010, **135**, 169–174.
38 S. Da Ros, M. D. Jones, D. Mattia, M. Schwaab, F. B. Noronha and J. C. Pinto, *Appl. Catal. A Gen.*, 2017, **530**, 37–47.
39 X. Huang, Y. Men, J. Wang, W. An and Y. Wang, *Catal. Sci. Technol.*, 2017, **7**, 168–180.

View Article Online
DOI: 10.1039/C8GC01211C